JOURNAL OF MATERIALS SCIENCE 27 (1992) 1969–1977

Analysis of the wedge-shaped damage zone in edge-notched polypropylene

J. SNYDER, A. HILTNER, E. BAER
Department of Macromolecular Science, and Center for Applied Polymer Research, Case Western Reserve University, Cleveland, OH 44106, USA

The irreversible deformation behaviour of polypropylene during sharp single-edge-notched tension testing has been studied as a function of temperature. Specimens were tested at room temperature, −20, −40, and −60 °C with photographs taken of the notch tip area during testing. Below T_g, a narrow wedge-shaped damage zone grew from the notch tip with increased stress. The damage zone length correlated with the ratio of applied stress to yield stress in agreement with the Dugdale model. The crack tip opening displacement (CTOD) was found to follow the predicted Dugdale CTOD when modified by using the secant modulus to account for viscoelasticity. The shape of the damage zone did not agree with the Dugdale model near the notch tip, but instead was found to follow a path of the minor principal stress trajectory. About T_g, the damage zone had a lower length-to-width ratio which no longer resembled the Dugdale model.

1. Introduction

When a material is subjected to a load in the presence of a flaw, crack or artificial notch, there is a high concentration of stress directly ahead of the notch tip. The response of a material to a locally high, multiaxial stress state determines the suitability of the material for many engineering applications. Polymers in general respond to these conditions by exhibiting a relatively large amount of reversible and irreversible deformation directly ahead of the notch, as compared with metals, ceramics or glasses.

The notched tension test is an effective tool in the study of the pre-fracture yielding behaviour of materials. In this test stresses are concentrated in the vicinity of the notch thereby causing local yielding, crack growth, and eventually catastrophic failure. In some cases a stable slow crack growth stage does not occur, and the failure process is dominated by pre-fracture events at the notch tip. This is the case with polypropylene, and the region of irreversible plastic deformation ahead of the notch, known as a damage zone, has been the subject of several recent studies [1–4].

The behaviour of polypropylene at low temperature in the presence of a sharp notch has been investigated by Chou *et al.* as part of a larger study of blends [1]. At −40 °C, a thin line damage zone appeared in polypropylene at approximately 50% of the fracture stress. As the stress increased, the damage zone grew in length, and the notch tip progressively blunted. By using the formalism of the elastic–plastic model of Dugdale [5], it was found that the length of the zone correlated with the ratio of the applied stress to the yield stress. Although there was success in modelling the damage zone length, no analysis of the width or shape of the damage zone in polypropylene was attempted. When the damage zone reached a critical length, the material fractured catastrophically without any apparent slow or stable crack growth. This type of pre-fracture damage behaviour was found to be characteristic of polypropylene at temperatures below the glass transition temperature, T_g.

Jang *et al.* in a study of the damage mechanisms of polypropylene as a function of temperature and strain rate [6], showed that at low temperatures and high strain rates crazing was the major irreversible deformation mechanism. Scanning electron microscopy was used to reveal the morphological details of crazes produced at −60 °C. At higher temperatures and lower strain rates, deformation was dominated by shear yielding and the craze-like features observed at −60 °C were not found.

Damage zones ahead of sharp notches have also been studied in several other polymer systems. In thin films or plane stress state, narrow damage zones are generally found to be one of two types; either single crazes or necked shear zones. In polymethyl methacrylate the damage zone consists of a single craze growing from the notch tip, and Döll *et al.* [7] and Brown and Ward [8] have successfully used the plane stress Dugdale model to describe the length of the single craze as well as its shape. When crazing is the deformation mechanism, the shape of the zone is relatively insensitive to thickness and the plane stress approach is applicable even in relatively thick sheet [8]. Thin films of polycarbonate, polysulphone and poly(vinyl chloride) also exhibit long narrow damage zones [9–11]. However, these are formed by necking through the thickness direction in the shear yielding mode of deformation. In these cases, the Dugdale

0022–2461

model was again used successfully to correlate the experimental damage zone lengths with the applied stress. Unlike polymers that craze, the behaviour of these shear yielding materials is highly sensitive to the thickness. As the thickness increases and the stress state shifts from plane stress to plane strain, the material fails in an apparently brittle manner [9].

In early work, the Dugdale model was used to describe the damage zones observed in notched steel tension specimens [5]. By using the Muskhelishvili's stress function to solve the elastic stress distribution ahead of the plastic region, Dugdale obtained an exact one-dimensional model solution for plane stress [12]. Goodier and Field subsequently refined this model by solving for the damage zone displacement in the tension direction to obtain the crack tip opening displacement [13]. This refined analysis works well in steels for predicting both the length and width of the damage zones [14, 15]. Although this model was originally applied to metals, it is a macroscopic model and is not concerned with the specific microdeformation mechanism. Its success in describing the behaviour of some polymers can be attributed to the similar one-dimensional deformation response of these materials to the complex triaxial stress state at the sharp notch.

The goal of this paper is to describe the damage zone evolution in polypropylene in notched tension at low temperatures, and subsequently to analyse quantitatively these zones as they develop ahead of the notch tip. The previous study showed that the Dugdale model predicts the length of the damage zone in polypropylene at low temperature [1], the current work extends the analysis to the damage zone width and shape. Furthermore, consideration will be given to development of the craze morphology [6] within the damage zone and its relationship to the local stress state.

2. Experimental procedure

2.1. Sample preparation

Polypropylene used in this investigation was obtained commercially in the form of a 6 mm thick extruded sheet. Dog-bone tension specimens, ASTM D638, Type 1, were cut from this sheet and 2.25 mm milled from each surface. With a skin layer of only 0.1 mm, this removed any possible skin effects in subsequent testing. Specimens were polished using 800, 1200 and 2400 grit wet sand paper giving all samples the same surface texture. Specimens to be used for subsequent microscopic examination were given an additional polishing with 5, 1 and 0.5 μm alumina powder. The test specimens had a gauge length of 60 mm with a 13 mm width and 1.2 mm final thickness. For notched testing, a single 1 mm edge notch was cut at room temperature using a fresh razor blade.

2.2. Mechanical testing

Tension testing was conducted on an Instron 1123 testing instrument equipped with a liquid nitrogen-cooled environmental chamber. Un-notched testing was carried out at a strain rate of 0.2% min^{-1}, and the notched testing at a crosshead speed of 0.1 mm min^{-1}. The pre-fracture damage ahead of the notch during loading was recorded using a 35 mm camera with a telephoto lens. This apparatus utilized a microscope objective lens to achieve a final print magnification of about $\times 75$, from which the data for damage zone analysis were obtained.

2.3. Microscopy

The damage zones of several notched specimens were examined using an Olympus optical microscope. Specimens that had been previously loaded and stopped prior to failure were observed using both transmitted and reflected light while being held in a stretcher at the same crack opening displacement as at the end of loading.

3. Results and discussion

3.1. Tension testing

Fig. 1 shows the results of tension testing of polypropylene at room temperature, − 20, − 40, and − 60 °C, with Table I, summarizing the tensile properties. The elastic modulus and yield strength both increased with decreasing temperature. These values

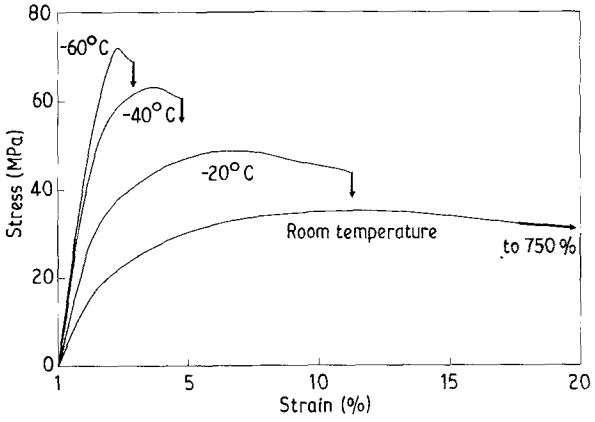

Figure 1 Stress–strain curves of polypropylene at various temperatures.

TABLE I Summary of the tensile properties of polypropylene as a function of temperature

	Temperature (°C)			
	Room	− 20	− 40	− 60
Tensile test				
Yield stress (MPa)	35.2	50.0	63.3	73.0
Tangent modulus (GPa)	1.42	2.55	4.11	4.39
Strain to failure (%)	750	11.4	4.9	2.8
Notched tensile test				
Max. notched stress (MPa)	31.4	39.6	47.9	51.9
Max. damage zone length (mm)	–	2.12	1.68	1.28
Analysis				
Secant modulus (GPa), from Fig. 8	–	1.19	2.07	3.36

agreed with the typically reported properties of polypropylene published by other authors [1, 6, 17]. At all temperatures the stress–strain curves showed a linear increase in stress with increasing strain to about 1.75% strain, followed by a non-linear increase in stress to the yield point. In this non-linear strain region, profuse "craze-like" stress whitening initiated and grew along the entire gauge length of the specimen.

A major change in the yielding behaviour was observed as the temperature was lowered through the T_g which was about 0 °C. At room temperature, specimens yielded with the formation of a stable neck, and a large degree of drawing preceded failure. Below the T_g, yielding was characterized by an intensification of the stress whitening in a localized region along the gauge length. The specimen then fractured where the intense stress whitening occurred in a relatively brittle manner without drawing. Accordingly as the temperature was decreased from room temperature to − 20 °C, the strain to failure showed a sharp decrease (Table I). At the lower temperatures of − 40 and − 60 °C the strain to failure continued to decrease but not as sharply.

3.2. Notched tensile testing

Fig. 2 shows the notched stress–extension curves of polypropylene for the same temperatures used in the un-notched tests. The changes in these curves with temperature were similar to those in the un-notched test, but the transition at the T_g was emphasized by the presence of a notch. At room temperature the notched stress–extension curve continued after stress instability was reached. This was accompanied by necking and drawing at the notch with stable crack growth prior to fracture. Below the T_g, the stress increased linearly at low sample extensions followed by a non-linear increase at higher extensions to a maximum stress where catastrophic failure occurred. The maximum stress prior to failure was much lower due to the presence of a notch, and the region of decreasing stress that followed the maximum stress in the un-notched case was absent.

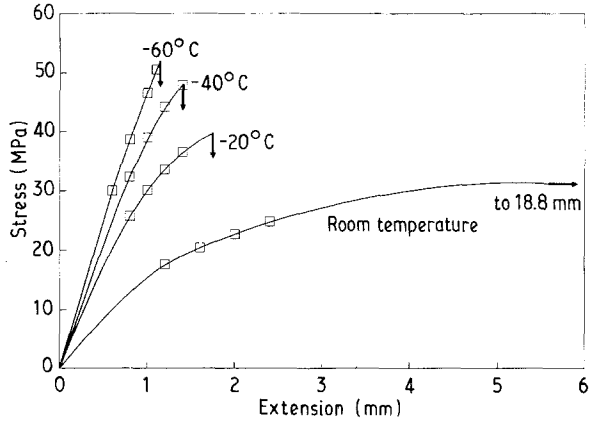

Figure 2 Notched stress–extension curves of polypropylene at four temperatures. The notch length was 1 mm, the location of photos taken of the damage zones is indicated.

Photographs of the notch tip area were taken at the positions indicated by the open squares in Fig. 2. Fig. 3a–d show the damage zone that developed ahead of the notch as the stress increased at each of the four temperatures. The damage zones were not clearly visible until the applied stress reached about 40% of the unnotched yield stress. At room temperature a flame-shaped damage zone grew from the notch tip. As the test proceeded this zone increased in both length and width until the stress reached a maximum at which point the sample necked at the notch tip. With continued stretching, a slow stable tearing type crack propagated from the notch tip to the edge of the sample with decreasing load. At temperatures below T_g (− 20, − 40 and − 60 °C) a narrow wedge-shaped damage zone grew from the notch tip. The zone grew with increasing stress primarily in length but also to a lesser extent in width. The ratio of the damage zone length to width increased with decreasing temperature. The highest length to width ratio was found at − 60 °C and the lowest at room temperature. Below T_g, there was also progressive blunting of the notch tip as the stress was increased followed by catastrophic fracture without crack growth. The damage zones observed at − 40 °C and room temperature closely matched those described by Chou *et al.* [1].

3.3. Analysis of the damage zones

3.3.1. Damage zone length

The growth of wedge-shaped damage zones has been treated by several authors in the mechanics literature. The size and shape of a damage zone is a function of both the materials response to local stresses and the specimen geometry. Several models of the stress state ahead of a sharp notch are available for the analysis [5, 17, 18]. The Dugdale model is applicable to the current problem because the wedge-shaped geometry of the damage zone in the model closely resembles the shape of the experimental zones [5]. Fig. 4 shows the Dugdale model for a single-edge-notched specimen. The model predicts the length of the damage zone as a function of the notch length, applied stress, and the un-notched yield strength of the material. The basic assumption in this model is that all the material in the damage zone is at the same stress, presumably the yield stress. The solution is a balance between the externally applied stress and the stress distribution ahead of the notch which includes both the plastic zone and the elastic stress distribution ahead of it. The predicted normalized damage zone length (C/A) is

$$\frac{C}{A} = \sec\left[\frac{\pi T}{2Y}\right] \quad (1)$$

where A is the notch length, T the applied stress, and Y the yield stress of the material [5].

Fig. 5 shows the measured damage zone length as a function of applied stress for the four test temperatures. The length of the zone and the stress level are normalized with respect to the notch length and the yield stress, respectively. The data for − 20, − 40 and − 60 °C showed very good agreement with the

Dugdale model. At room temperature, the length-to-width ratio of the damage zone was lower and the shape no longer resembled the Dugdale model. Analysis of the room-temperature damage zone therefore required a different approach, and only low-temperature data were analysed further.

The success of the Dugdale model in describing the length of the low-temperature damage zones was attributed to the validity of the assumption that the stress level within the damage zone was at a single average value, namely the yield stress. Another important reason for success was that damage to polypropylene below T_g was caused mainly by stresses in the y-direction, thus giving a sharp wedge shape to the damage zone. This was consistent with crazing being the major deformation mechanism of polypropylene at low temperatures [6].

3.3.2. Damage zone width

Another important aspect of the Dugdale model is the contribution of Goodier and Field who further developed the model by solving the displacement of the notch and damage zone in the loading direction [13]. The predicted displacement, $2v$, of the notch surfaces and the damage zone width (y-direction) as a function of distance, x, measured from the sample edge, and notch length, A, follows the relation

$$v(x, A) = \frac{C}{\pi}\frac{Y}{E}\left\{\cos(\theta)\ln\left[\frac{\sin^2(\beta - \theta)}{\sin^2(\beta + \theta)}\right] + \cos(\beta)\ln\left[\frac{(\sin\beta + \sin\theta)^2}{(\sin\beta - \sin\theta)^2}\right]\right\} \quad (2)$$

where $\beta = \pi T/2Y$, $\theta = \cos^{-1}(x/A)$, E is the elastic modulus, and C is calculated from Equation 1 [13]. Using this relationship the crack tip opening displacement (CTOD) is defined as twice the value of v at $x = A$ (see Fig. 4). At this position, Equation 2 approaches

$$\text{CTOD} \equiv 2v(A, A) = \frac{8A}{\pi}\frac{Y}{E}\ln\left[\sec\left(\frac{\pi T}{2Y}\right)\right] \quad (3)$$

The measured CTOD at $-40\,^{\circ}C$ was about double that predicted by Equation 3 as plotted in Fig. 6. The magnitude of the CTOD in Equation 3 is dependent on the applied stress, yield stress, modulus and geometric constants, two of which, the modulus and yield stress, are materials parameters. Only one material parameter, the yield stress, is required in Equation 1, which satisfactorily predicted the length of the damage zone. It was, therefore, reasonable to reconsider the value of the modulus used in the CTOD calculations. The modulus used in the calculation plotted in Fig. 6 was the tangent modulus obtained from the initial slope of the un-notched stress–strain curve. In metals, for which the models were developed, the ratio of the

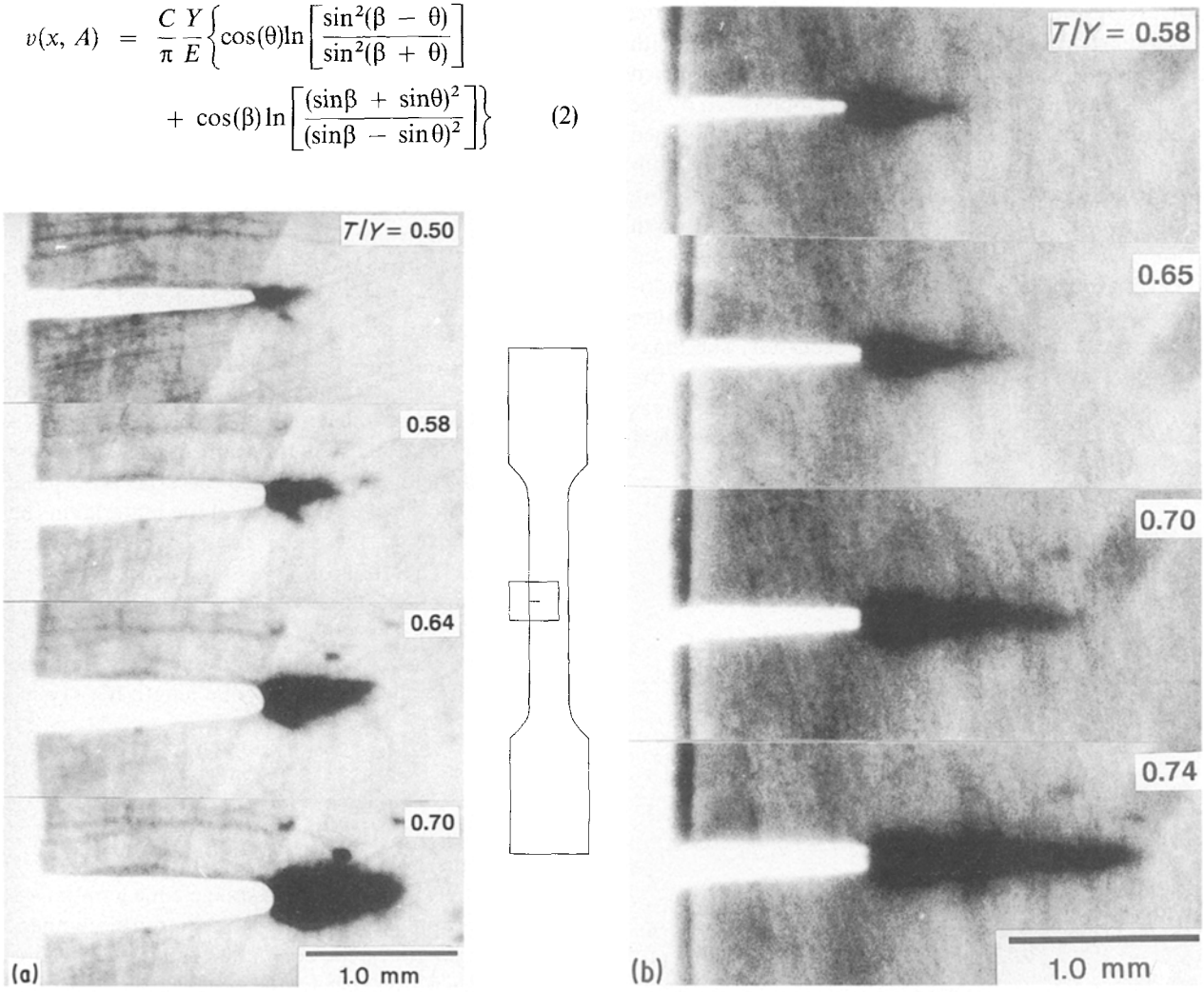

Figure 3 Photographs of the notched tensile test at (a) room temperature, (b) $-20\,^{\circ}C$, (c) $-40\,^{\circ}C$ and (d) $-60\,^{\circ}C$ showing the growth of the damage zones at four stress levels.

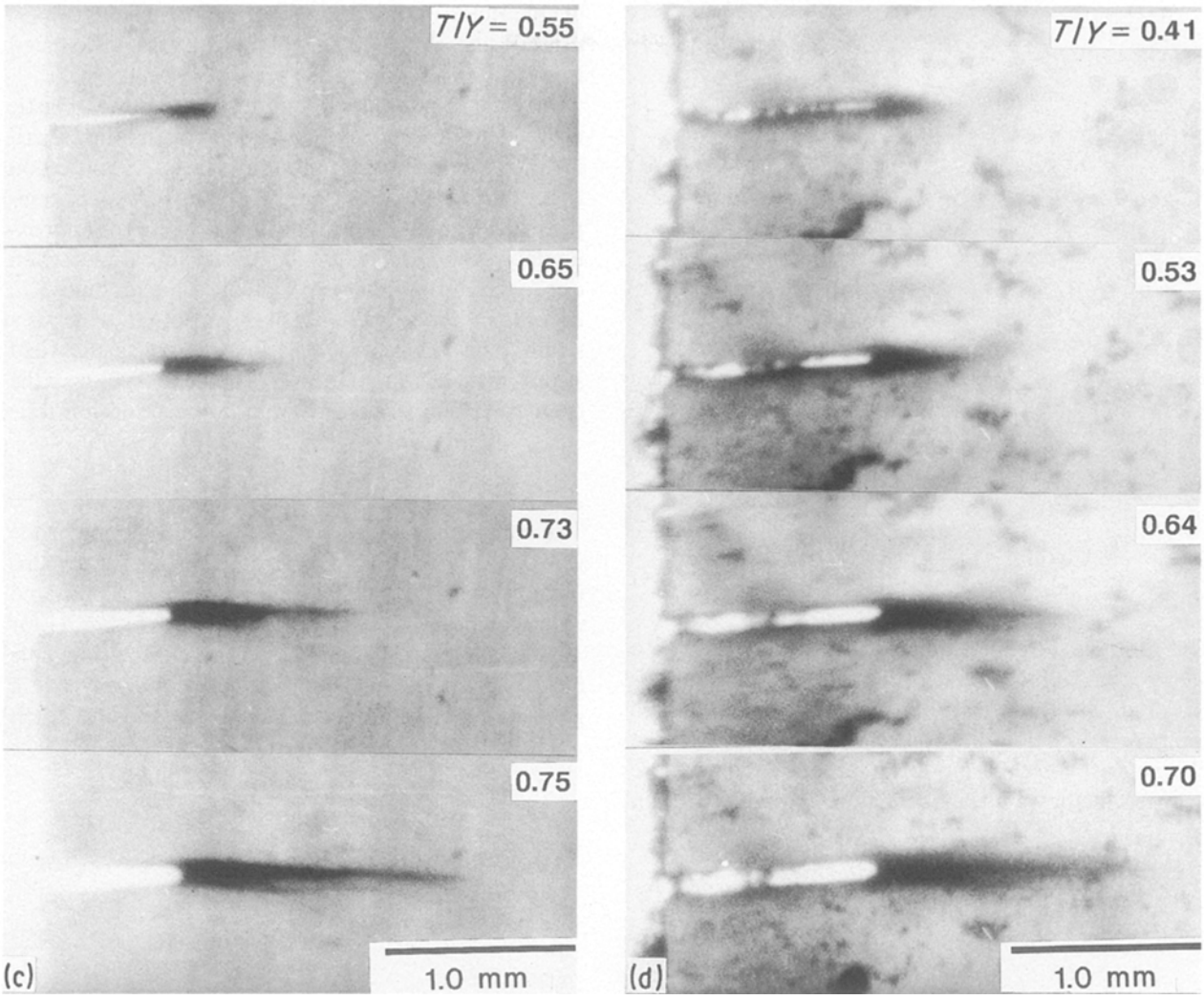

Figure 3 Continued.

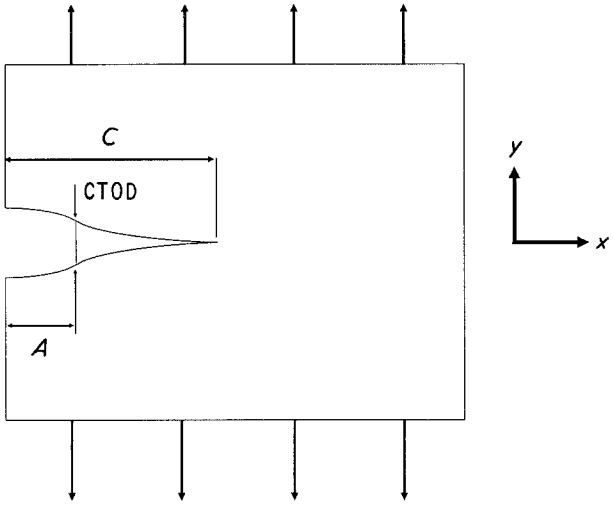

Figure 4 Schematic drawing of the Dugdale model for the damage zone ahead of a single-edge notch.

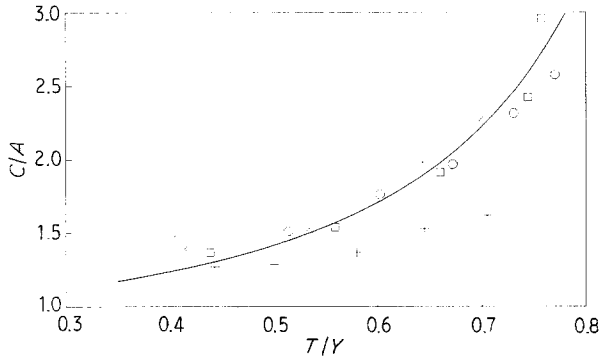

Figure 5 Plot of the normalized damage zone length, C/A, versus normalized stress, T/Y, for data measured at (×) − 60, (□) − 40, (○) − 20 °C and (+) room temperature. Also shown is the predicted length from the Dugdale model (—).

yield stress to the tangent modulus is close to the strain at yielding because of high linearity up to the yield point. This is generally not the case with polymers where high non-linearity causes the yield strain to be much higher than in metals. Under these circumstances a more appropriate choice of modulus is a secant modulus [19]. The difference between the initial tangent modulus and one of many possible secant moduli is demonstrated in Fig. 7a with an experimental stress–strain curve for polypropylene together with the resulting ideal elastic–plastic stress–strain curve in Fig. 7b.

If a unique secant modulus can describe the CTOD data for all stress levels, then from Equation 3, a plot

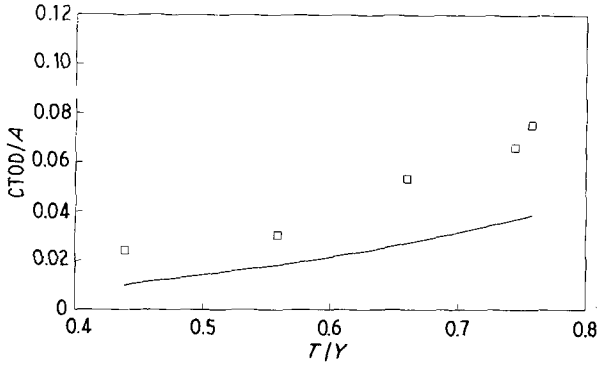

Figure 6 Plot of the normalized crack tip opening displacement CTOD/A versus normalized stress at $-40\,^{\circ}C$, along with (—) the predicted CTOD/A from the Goodier and Field equation.

of

$$\frac{\text{CTOD}}{A} \text{ versus } \frac{8Y}{\pi} \ln\left[\sec\left(\frac{\pi T}{2Y}\right)\right] \tag{4}$$

will produce a straight line through the origin with a slope equal to the inverse of the unique secant modulus. Fig. 8 shows this plot for each of the three temperatures below T_g. The plots were linear and the characteristic secant modulus for each temperature was obtained by a linear regression through the origin (Table I). Fig. 9 shows the CTOD data for the temperatures below T_g together with the curves calculated from Equation 3 using the secant modulus.

In Fig. 10 the corresponding ideal elastic–plastic curve, determined from the yield stress and the experimentally derived secant modulus, is superimposed on the un-notched stress–strain curve for each temperature. The yield strain on the ideal curves approximately coincided with the craze initiation strain observed during the experiment. The modulus, E, appears in Equation 3 only in the ratio Y/E which is a strain. The value of Y/E is interpreted as the yield strain in metals [13], in polypropylene Y/E_s was the craze initiation strain in the un-notched tension test.

3.3.3. Damage zone shape

The complete profiles of the notch and damage zone were calculated from Equation 2 using the experimentally derived secant modulus. These are compared with sketches of the actual damage zones in Fig. 11 for -20, -40 and $-60\,^{\circ}C$. Although the Dugdale model with the Goodier and Field equation gave a good fit with the damage zone length and the notch

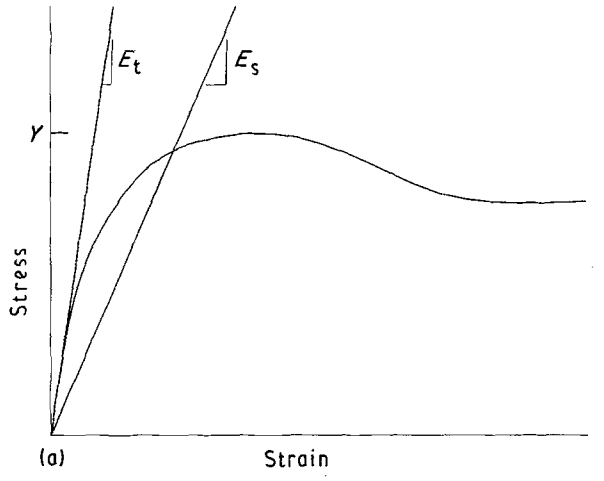

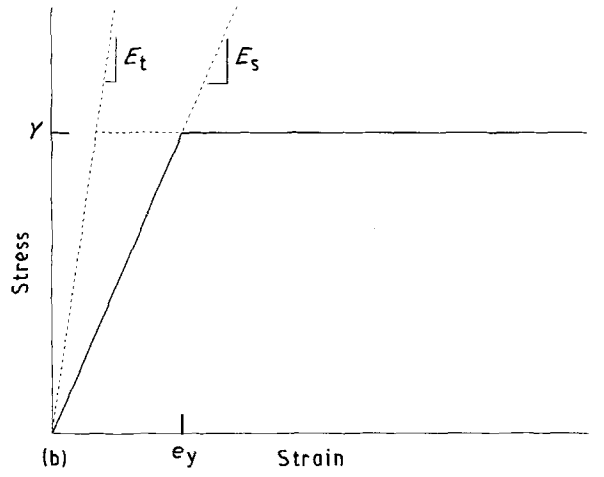

Figure 7 (a) The secant modulus construction in a typical stress–strain curve. (b) The idealized elastic–plastic stress–strain curve which uses the secant modulus.

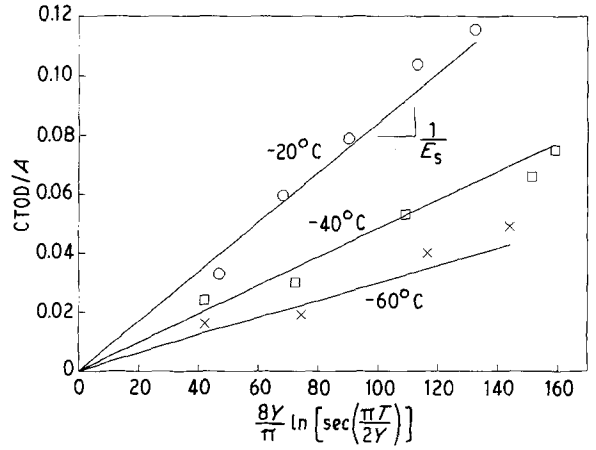

Figure 8 Plot of the CTOD/A to determine the secant modulus used in the Goodier and Field equation for data obtained at (×) -60, (□) -40, and (○) $-20\,^{\circ}C$.

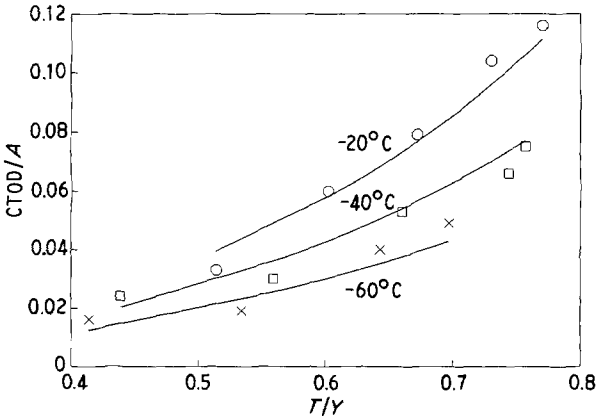

Figure 9 Plot of the experimental CTOD/A versus T/Y for (○) -20, (□) -40, (×) $-60\,^{\circ}C$, along with (—) the modified Goodier and Field predictions.

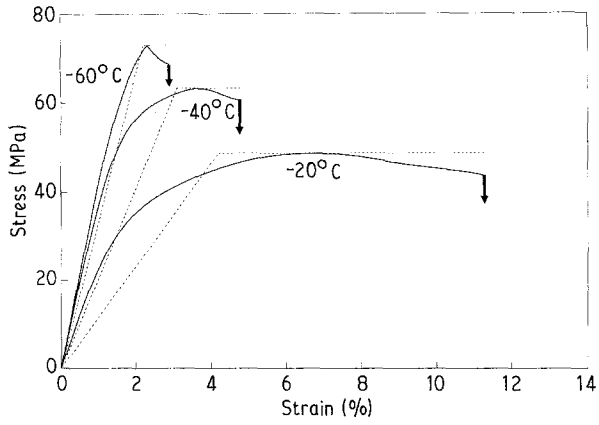

Figure 10 The un-notched stress–strain curves with an overlay of the elastic–plastic model obtained from the calculated secant modulus and the yield stress.

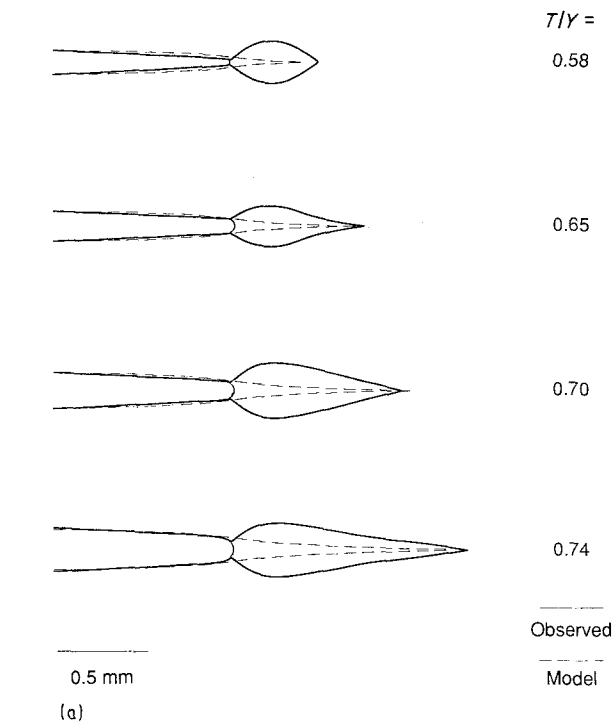

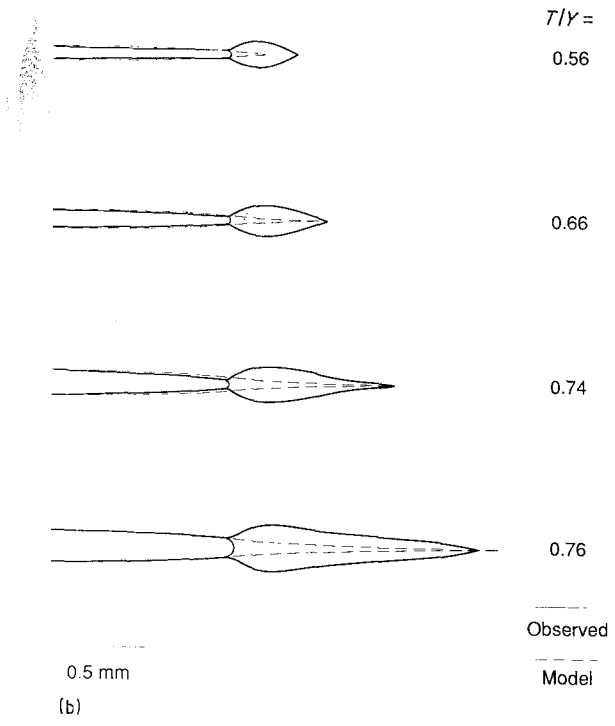

opening displacement, the model did not accurately describe the shape of the damage zone immediately ahead of the blunted notch tip. Instead of tapering in a wedge-shape, the zone widened at the notch root before gradually becoming more narrow. The failure of this aspect of the Dugdale analysis stemmed from the one-dimensional nature of the stress distribution used in formulating the model. In the Dugdale model and the Goodier and Field equation, only the stress distribution in the direction of the applied stress (y-direction) is considered. However, near a notch tip the real stress fields are multidirectional, and the stresses perpendicular to the externally applied load approach the same level as those parallel to it [18].

Crazing has been reported to be the primary microdeformation mechanism for polypropylene at temperatures below the glass transition [2, 6, 20]. Work on other polymers that craze has shown that craze growth follows a path perpendicular to the direction of the maximum local principal stress [21]. A trajectory plot of the local principal stress directions was constructed using a method similar to that of Chabaat [21], taking into account Creager and Paris's correction for notch-tip blunting [22]. In Fig. 12 the major principal stress trajectories are plotted as the dashed lines with the minor principal stress trajectories plotted as solid lines. When one of the minor stress trajectories was superimposed on a magnified photograph of the damage zone at $-40\,^{\circ}C$ and a relative stress level of 0.76, Fig. 13, it was evident that the macroscopic damage zone shape was described by a principal stress trajectory.

To view the damage zone at higher magnification, a specimen was pulled to a relative stress level of 0.66 at

Figure 11 Drawings of the damage zone shape at (a) $-20\,^{\circ}C$, (b) $-40\,^{\circ}C$ and (c) $-60\,^{\circ}C$ comparing the experimental observation (—) with the zone predicted by the Dugdale, and Goodier and Field models (– – –).

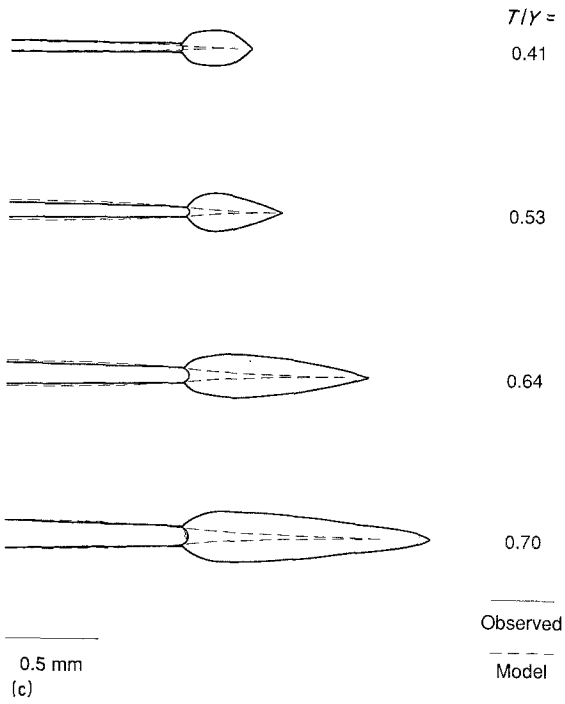

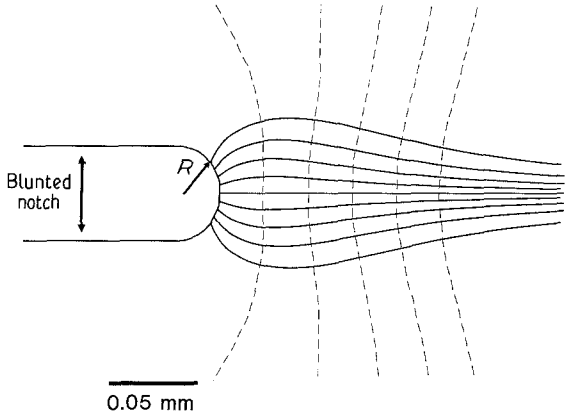

Figure 12 Maximum and minimum principal stress trajectories ahead of a blunted notch with tip radius, R, using Chabaat's method [21].

– 40 °C, held for 30 min and unloaded, then pulled in a stretcher at room temperature to the same CTOD and observed under an optical microscope. The damage zone was found to be composed of numerous crazes that all followed minor principal stress trajectories (Fig. 14). The large number of crazes was the principal difference between the damage zone of polypropylene and that of glassy polymers such as polymethyl methacrylate where a single craze constitutes the damage zone [7], and the craze profile follows the shape of the Dugdale model very closely.

4. Conclusions

The results of this investigation show that the damage zone in polypropylene at low temperatures consists of

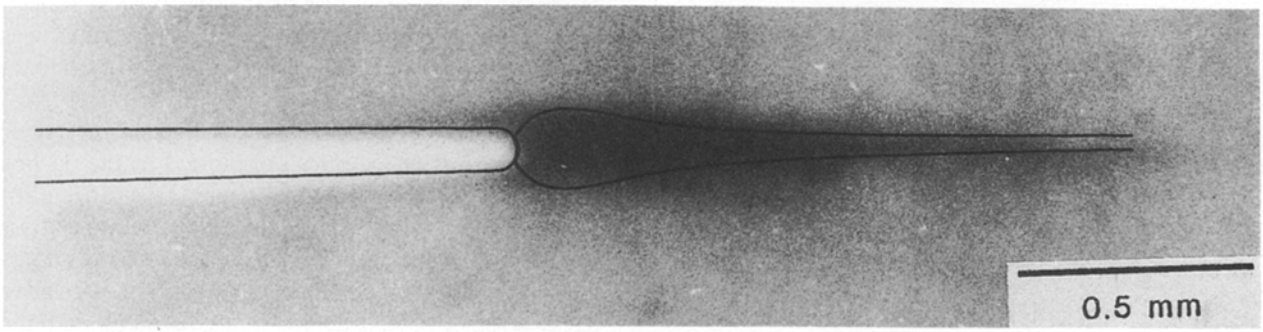

Figure 13 Magnified view of a damage zone with one of the stress trajectories overlaid. Temperature was – 40 °C, and $T/Y = 0.76$.

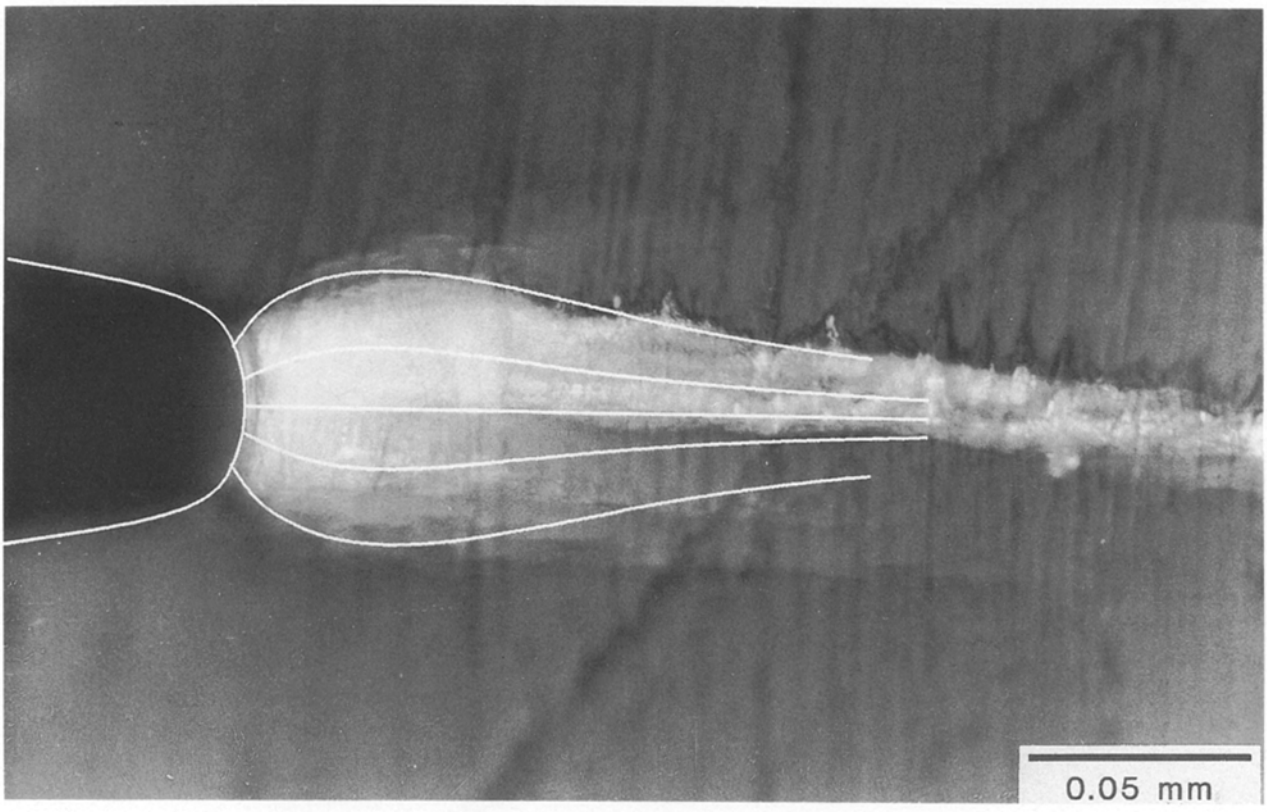

Figure 14 Optical micrograph of the damage zone produced at – 40 °C showing the craze structure with several stress trajectories overlaid (polarized light).

multiple crazes which develop ahead of the notch in the most highly stressed areas. The following conclusions are drawn from the mechanical analysis of the damage zone.

1. The damage zone length follows the Dugdale model very closely at temperatures below T_g. Above T_g, the length to width ratio of the damage zone becomes much lower and the model does not apply.

2. The Goodier and Field analysis accurately estimates the experimental CTOD from materials parameters when a secant modulus is used to account for viscoelasticity.

3. The shape of the damage zone does not follow the Dugdale model near the notch tip due to the real two-dimensional stress distribution which is not taken into account in the one-dimensional Dugdale model. The shape of the damage zone is determined by the path of craze growth which follows the maximum principal stress trajectories.

Acknowledgement

The authors thank The National Science Foundation, Polymers Program, grant number DMR87-13041, and the Army Research Office, grant number DAAL03-88K-0097, for their generous support of this work.

References

1. C. CHOU, K. VIJAYAN, D. KIRBY, A. HILTNER and E. BAER, *J. Mater. Sci.* **23** (1988) 2533.
2. K. FRIEDRICH, *Colloid Polym. Sci.* **64** (1978) 103.
3. *Idem., ibid.* **66** (1979) 299.
4. I. NARISAWA, *Polym. Engng Sci.* **27** (1987) 41.
5. D. S. DUGDALE, *J. Mech. Phys. Solids* **8** (1960) 100.
6. B. Z. JANG, D. R. UHLMANN and J. B. VAN DER SANDE, *Polym. Engng Sci.* **25** (1985) 98.
7. W. DÖLL, L. KNÖCÖL and M. G. SCHINKER, *Polymer* **24** (1983) 1213.
8. H. R. BROWN and I. M. WARD, *ibid.* **14** (1973) 469.
9. N. J. MILLS, *Engng Fract. Mech.* **6** (1974) 537.
10. H. F. BRINSON, *Exp. Mech.* **10** (1970) 72.
11. I. NARISAWA, M. ISHIKAWA and H. OGAWA, *J. Mater. Sci.* **15** (1980) 2059.
12. D. C. DRUCKER and J. R. RICE, *Engng Fract. Mech.* **1** (1970) 577.
13. J. N. GOODIER and F. A. FIELD, in "Fracture of Solids", edited by D. C. Drucker and J. J. Gilman (Interscience, New York, 1963) p. 103.
14. G. T. HAHN and A. R. ROSENFIELD, *Acta Metall.* **13** (1965) 293.
15. B. J. SCHAEFFER, H. W. LIU and J. S. KE, *Exp. Mech.* **11**, (1971) 172.
16. B. HARTMANN, G. F. LEE and W. WONG, *Polym. Engng Sci.* **27** (1985) 823.
17. G. R. IRWIN and J. A. KIES, *Weld. J. Res. Suppl.* **33** (1954) 1935.
18. H. TADA, P. PARIS, G. R. IRWIN, "The Stress Analysis of Cracks Handbook" (Del Research Corporation, Hellertown, PA, 1978).
19. E. BAER, J. R. KNOX, T. J. LINTON and R. E. MAIER, *SPE J.* **16** (1960) 396.
20. K. D. PAE, D. R. MORROW and J. A. SAUER, in "Proceedings of the first international conference on fracture", Vol. **2**, edited by T. Kokobori, T. Kawasaki and J. L. Swedlow (Japanese Society for Strength and Fracture of Materials, Sendai, Japan, 1966) p. 1229.
21. M. CHABAAT, *Int. J. Fract. Mech.* **37** (1988) R47.
22. M. CREAGER and P. PARIS, *ibid.* **3** (1967) 247.

Received 22 May
and accepted 3 June 1991